Cancer Science
Japanese Cancer Association JCA
Open Access

Enhanced efficacy against cervical carcinomas through polymeric micelles physically incorporating the proteasome inhibitor MG132

Yoko Matsumoto,[1] Yuichiro Miyamoto,[1] Horacio Cabral,[2] Yu Matsumoto,[3] Kazunori Nagasaka,[1] Shunsuke Nakagawa,[4] Tetsu Yano,[5] Daichi Maeda,[6] Katsutoshi Oda,[1] Kei Kawana,[1] Nobuhiro Nishiyama,[7] Kazunori Kataoka[2,8,9,10] and Tomoyuki Fujii[1]

[1]Department of Obstetrics and Gynecology, Faculty of Medicine; [2]Department of Bioengineering, Graduate School of Engineering; [3]Department of Otolaryngology, Faculty of Medicine, The University of Tokyo; [4]Department of Obstetrics and Gynecology, Faculty of Medicine, The University of Teikyo; [5]Department of Obstetrics and Gynecology, National Center for Global Health and Medicine, Tokyo; [6]Department of Cellular and Organ Pathology, Graduate School of Medicine, Akita University, Akita; [7]Polymer Chemistry Division, Chemical Resources Laboratory, Tokyo Institute of Technology, Yokohama; [8]Center for Disease Biology and Integrative Medicine, Graduate School of Medicine; [9]Department of Materials Engineering, Graduate School of Engineering, The University of Tokyo, Tokyo; [10]Innovation Center of Nanomedicine, Kawasaki Institute of Industry Promotion, Kawasaki, Japan

Key words

Antineoplastic agents, benzyloxycarbonylleucyl-leucyl-leucine aldehyde, drug delivery system, nanomedicine, uterine cervical neoplasms

Correspondence

Shunsuke Nakagawa, Department of Obstetrics and Gynecology, Faculty of Medicine, The University of Teikyo, 2-11-1 Kaga, Itabashi-ku, Tokyo 173-8606, Japan.
Tel: +81-3-3964-8736; Fax: +81-3-3481-8283;
E-mail: nakagawas-tky@umin.ac.jp
and
Kazunori Kataoka, Department of Bioengineering, Graduate School of Engineering, The University of Tokyo, 7-3-1 Hongo, Bunkyo-ku, Tokyo 113-8656, Japan
Tel: +81-3-5841-7138; Fax: +81-3-5841-7139;
E-mail: kataoka@bmw.t.u-tokyo.ac.jp

Funding Information

Ministry of Education, Culture, Sports, Science and Technology of Japan; Banyu Foundation; Japan Science and Technology Agency; Japan Agency for Medical Research and Development.

Received October 24, 2015; Revised March 2, 2016; Accepted March 8, 2016

Cancer Sci **107** (2016) 773–781

doi: 10.1111/cas.12926

Treatment of recurrent or advanced cervical cancer is still limited, and new therapeutic choices are needed for improving prognosis and quality of life of patients. Because human papilloma virus (HPV) infection is critical in cervical carcinogenesis, with the *E6* and *E7* oncogenes of HPV degrading tumor suppressor proteins through the ubiquitin proteasome system, the inhibition of the ubiquitin proteasome system appears to be an ideal target to suppress the growth of cervical tumors. Herein, we focused on the ubiquitin proteasome inhibitor MG132 (carbobenzoxy-Leu-Leu-leucinal) as an anticancer agent against cervical cancer cells, and physically incorporated it into micellar nanomedicines for achieving selective delivery to solid tumors and improving its *in vivo* efficacy. These MG132-loaded polymeric micelles (MG132/m) showed strong tumor inhibitory *in vivo* effect against HPV-positive tumors from HeLa and CaSki cells, and even in HPV-negative tumors from C33A cells. Repeated injection of MG132/m showed no significant toxicity to mice under analysis by weight change or histopathology. Moreover, the tumors treated with MG132/m showed higher levels of tumor suppressing proteins, hScrib and p53, as well as apoptotic degree, than tumors treated with free MG132. This enhanced efficacy of MG132/m was attributed to their prolonged circulation in the bloodstream, which allowed their gradual extravasation and penetration within the tumor tissue, as determined by intravital microscopy. These results support the use of MG132 incorporated into polymeric micelles as a safe and effective therapeutic strategy against cervical tumors.

Invasive cervical cancer remains a leading cause of death among women with annual deaths estimated at 275 000 worldwide and an age-standardized mortality rate of 15.2/100 000, ranking it the second highest cause of death from all cancers for women.(1) Moreover, prognosis of advanced or recurrent patients remains poor with a 1-year survival rate of 15–20%.(2) While the recent approval of vaccines against some high-risk HPVs will greatly impact on the incidence of cervical cancer by preventing HPV infection and development of cancer, new therapeutic options are still needed for improving survival and quality of life of patients with advanced and/or recurrent cervical tumors.

After HPV infection, the *E6* and *E7* oncogenes of HPV have been shown to be key for carcinogenesis, being sufficient for immortalizing cultured primary keratinocytes.(3,4) The high-risk HPV E6 is combined with ubiquitin-protein ligase E6AP, inactivating and degrading tumor suppressor proteins (e.g., p53 and hScrib) through the UPS.(5) Indeed, as the degradation of tumor suppressor proteins by proteasomes is a significant step in the progress of cervical cancer, previous reports indicated some proteasome inhibitors might have antitumor effects against cervical tumors.(6,7) Moreover, the recent clinical approval of proteasome inhibitors by the FDA for the treatment of relapsed and refractory multiple myeloma(8) indicates their potential for designing translational therapies. However, despite their high efficacy, proteasome inhibitors are associated with strong side-effects, including bone marrow suppressions like neutropenia and low platelets,(9,10) and even fatal toxicities, such as interstitial

pneumonia and cardiac dysfunctions.[10] Therefore, novel therapeutic strategies for providing safe, selective, and efficient inhibition of the proteasome are required for improved systemic chemotherapy for cervical cancer.

Application of nano-scaled carriers has the potential for selectively delivering proteasome inhibitors to their site of action, reducing non-specific distribution in normal tissues, and enhancing the accumulation in tumor based on the EPR effect, that is, the increased permeability of tumor vasculature and the impaired lymphatic drainage of tumor tissues.[11–13] Thus, the accumulation of nanocarriers in tumor tissues involves their extravasation through the openings in the leaky tumor vasculature, followed by their penetration and retention within the tumor. Among nano-scaled carriers, polymeric micelles, that is, core-shell nanoassemblies of block copolymers encapsulating therapeutic molecules in their core, have been reported to have high targeting efficiency for solid tumors with decreased side-effects.[13,14] Polymeric micelles have a prolonged half-life in the bloodstream, which can facilitate their accumulation in tumor tissue, as long-circulating nanocarriers can repeatedly flow through the tumor vasculature. Their relatively small size, in the <100-nm range, allows them to reach deeply into tumor tissues. Several clinical trials of polymeric micelles incorporating anticancer drugs are ongoing.[15–17] Thus, in the present study, we prepared polymeric micelles physically incorporating MG132 in their core through self-assembly of the amphiphilic block copolymer PEG-*b*-PBLG (Fig. 1), and their activity was evaluated *in vivo* against xenograft models of human cervical cancer, including HPV-positive HeLa and CaSki cells, as well as HPV-negative C33A cells. The mechanisms of therapeutic activity were studied by fluorescent immunohistochemistry, intravital microscopy, and histology. Our results indicate a safe and potent activity profile for MG132/m against human cervical cancers.

Materials and Methods

Materials. γ-Benzyl L-glutamate was purchased from Chuo Kaseihin (Tokyo, Japan) and MG132 (Z-Leu-Leu-Leu-al) was purchased from Sigma-Aldrich (St. Louis, MO, USA). Bis (trichloromethyl) carbonate (triphosgene) was purchased from Tokyo Kasei Kogyo (Tokyo, Japan). Both DMF and DMAc were purchased from Wako Pure Chemicals Industries (Tokyo, Japan). α-Methoxy-ω-amino-polyethylene glycol (CH_3O-PEG-NH_2; molecular weight, 12 000 Da) was purchased from NOF (Tokyo, Japan). BODIPY TR cadaverine was purchased from Invitrogen (Carlsbad, CA, USA). Blocking One Buffer was purchased from Nacalai Tesque (Tokyo, Japan), and DMEM was purchased from Sigma-Aldrich. Anti-hScrib and anti-p53 were purchased from Santa Cruz Biotechnology (Santa Cruz, CA, USA). Alexa Fluor 488-conjugated donkey anti-mouse IgG and Alexa Fluor 555-conjugated goat anti-rabbit IgG were purchased from Invitrogen.

Animals. Five-week-old female C.B-17/lcr-*scid/scid*Jcl mice were purchased from CLEA Japan (Tokyo, Japan) for the *in vivo* antitumor activity assay. Five-week-old female BALB/c wild-type mice, for the toxicity experiment, and 7-week-old female BALB/c nu/nu mice, for intravital imaging, were purchased from Charles River Japan (Kanagawa, Japan). All the animal procedures were carried out in accordance with The University of Tokyo (Tokyo, Japan) guidelines for the care and use of experimental animals, which meet the ethical standards required by law and also comply with the guidelines for the use of experimental animals stated by The University of Tokyo.

Cell lines. The human cervical carcinoma cell lines HeLa, CaSki, and C33A, were purchased from ATCC (Manassas, VA, USA). HeLa (HPV-18-positive) and CaSki (HPV-16-positive) contain wild-type p53. C33A is an HPV-negative cell line and expresses mutant p53 mRNA.[18] HeLa cells stably expressing GFP in the nucleus (HeLa-H2B-GFP) were generously supplied by Dr. Teru Kanda (Aichi Cancer Center Research Institute, Aichi, Japan).[19] Cells were cultured in DMEM containing 10% FBS in a humidified atmosphere containing 5% CO_2 at 37°C and were detached with 0.05% trypsin/0.5 mM EDTA in PBS.

Polymer preparation. The PEG-*b*-PBLG copolymer was prepared as previously reported.[20] Briefly, the copolymer was prepared by polymerization of *N*-carboxy anhydride of γ-benzyl L-glutamate initiated by CH_3O-PEG-NH_2 in DMF. The molecular weight distribution of PEG-*b*-PBLG was determined to be 1.06 by gel permeation chromatography (column, TSK-gel $G3000_{HHR}$, $G4000_{HHR}$ [Tosoh, Yamaguchi, Japan]; eluent, DMF with 10 mM LiCl; flow rate, 0.8 mL/min; detector, refractive index; temperature, 25°C). The polymerization degree of PEG-*b*-PBLG was determined to be 40 by comparing the proton ratios of methylene units in PEG ($-OCH_2CH_2-$, δ = 3.7 p.p.m.) and phenyl groups of PBLG ($-CH_2C_6H_5$, δ = 7.3 p.p.m.) in ^{1}H-NMR measurement (EX270 [JEOL, Tokyo, Japan] solvent, DMSO-d_6; temperature, 70°C).

Preparation and characterization of MG132/m. MG132-loaded micelles were self-assembled by mixing 0.5 mg MG132 and

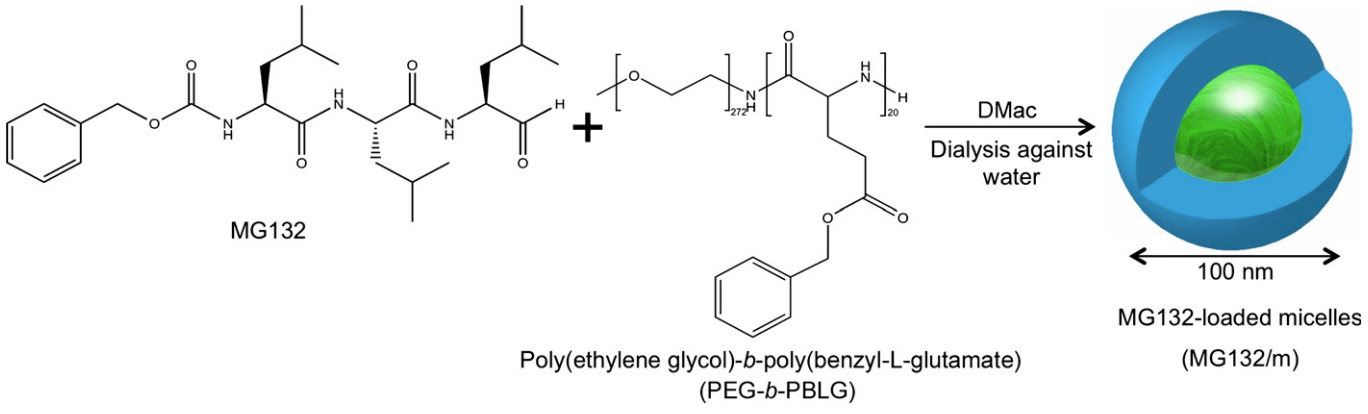

Fig. 1. Formation of MG132-loaded polymeric micelles (MG132/m). DMac, dimethyl acetamide.

1 mg PEG-*b*-poly (γ-benzyl-L-glutamate) in 1 mL DMAc, and dialyzing against water (MWCO, 1000 Da). The prepared micelles were further purified and concentrated by ultrafiltration (MWCO, 30 000 Da). The size distribution of MG132/m was evaluated by DLS at 25°C, using the Zetasizer Nano ZS90 (Malvern Instruments, Malvern, UK). The loading of MG132 in the micelles was determined by UV spectroscopy at 250 nm after freeze-drying 1 mL MG132/m, redissolving in DMAc, and dialyzing against 10 mL DMAc for 24 h. To prepare micelles incorporating fluorescent-labeled MG132, MG132 was firstly reacted with BODIPY TR cadaverine (Invitrogen) in DMAc and purified using a Sephadex LH20 column (Amersham Biosciences, Little Chalfont, UK). The MG132-BODIPY-TR was then loaded in polymeric micelles following the method described above.

The stability of MG132/m was evaluated in physiological conditions. For this, MG132/m (2 mg/mL on a micelle base) were mixed with DMEM cell culture media containing 10% FBS. The mixture was incubated in the dark at 37°C. At established time points, MG132/m were diluted 10 times in water and their size was evaluated by DLS. The drug release rate of MG132/m was studied under similar conditions by ultrafiltrating the samples at defined time points (ultrafiltration MWCO, 100 000 Da), diluting the ultrafiltrate 10 times in DMSO and checking by HPLC (eluent, MeOH:1% acetic acid, 9:1). At all time points (0–72 h), no drug peak could be detected, indicating no drug leakage from the micelles.

Antitumor activity assay. C.B-17/Icr-*scid/scid*Jcl mice were inoculated s.c. with HeLa, CaSki, or C33A (1×10^7 cells). Tumors were allowed to grow for 1 week. Mice were killed and tumors were removed. Tumors were then cut into 2-mm diameter pieces and s.c. transplanted in C.B-17/Icr-*scid/scid*Jcl mice ($n = 6$ per group). One week after inoculation, mice were treated with i.v. injection of saline (control), MG132 (1 mg/kg/dose), or MG132/m (1 mg/kg/dose on a MG132 base) twice a week for 4 weeks, as indicated in Figure 3. The volume (V) of tumors was measured before every injection, as estimated using equation $V = a \times b^2/2$ where a and b are major and minor axes of the tumor measured by a caliper, respectively.

Toxicity study. The toxicities of MG132/m were evaluated using three groups of wild-type BALB/c mice ($n = 4$ per group). They were treated with 1 mg/kg MG132 or MG132/m or control for 4 weeks every 3–4 days. Mice weight was measured on every injection day. After seven injections, the tissues responsible for nanoparticle elimination and where MG132/m highly accumulated, that is, liver, kidney, and spleen, were excised and histopathologically examined. Organs were embedded in paraffin blocks, sliced, and placed onto glass slides. After H&E staining, photographs were taken using an optical microscope and a pathological analysis was carried out.

Intravital microscopy. Intravital real-time confocal laser scanning microscopy for video-rate analysis of pharmacokinetics was carried out using a Nikon A1R confocal laser scanning microscope system attached to an upright ECLIPSE FN1 (Nikon, Tokyo, Japan).[21] The A1R incorporates both a conventional galvano scanner and a high-speed resonant scanner. The resonant scanner allows an acquisition speed of 30 frames/s while maintaining a high resolution of 512 × 512 scanned points. Mice were anesthetized with 2.0–3.0% isoflurane (Abbott Japan, Tokyo, Japan) using a Univentor 400 Anesthesia Unit (Univentor, Zejtun, Malta). Mice were then subjected to lateral tail vein catheterization with a 30-gauge needle (Becton Dickinson, Franklin Lakes, NJ, USA) connected to a non-toxic, medical grade polyethylene tube (Natsume Seisakusho, Tokyo, Japan). The difference in the pharmacokinetics of free fluorescent-labeled MG132-BODIPY TR and micelle-loaded fluorescent-labeled MG132 (MG132-BODIPY TR/m) was analyzed by intravital real-time confocal laser scanning microscopy in 7-week-old female BALB/c nude mice inoculated s.c. with HeLa-H2B-GFP cells. The tumors were allowed to mature until the size reached 3 mm in diameter. The signal from MG132-BODIPY TR and MG132-BODIPY TR/m was followed in the blood vessels and in the tumor interstitium to analyze their difference in blood circulation and accumulation into the tumor by visual image. Video acquisition at a speed of 30 frames/s was performed for the first 10 min after injection followed by time-lapse imaging every 5 min. MG132 or MG132/m were given at 100 μg/dosage through a tail vein catheter 10 s after video acquisition was initiated.

Immunofluorescence. The xenograft tumors were taken from mice 24 h after injection of control (vehicle), free MG132, or MG132/m. Tumors were frozen in optimal cutting temperature compound (Sakura Finetec Japan, Tokyo, Japan). The embedded tissues were cut on a cryostat and fixed with PBS containing 4% paraformaldehyde. The tissues were sequentially incubated with anti-p53 or anti-hScrib antibodies and appropriate secondary antibodies. Then the tissues were counterstained and analyzed under a fluorescence microscope (Olympus BX50; Olympus, Tokyo, Japan). Apoptotic cells were detected by the DeadEnd Fluorometric TUNEL system (Promega, Madison, WI, USA). The fluorescence signal in the tissues was quantified using the ImageJ (http://rsb.info.nih.gov/ij/download.html) program, and the statistical significance of these results was evaluated by Student's *t*-test.

Biodistribution. The mice used for intravital microscopy analysis were killed 24 h after injection of free MG132 or MG132/m. Tumors and organs (ear lobe, brain, lung, leg muscle, liver, spleen, and kidney) were taken and analyzed under confocal laser microscope (LSM510 Meta; Carl Zeiss, Jena, Germany). Six ROI in the tumor and organs were randomly selected and average fluorescent intensities were measured and analyzed.

***In vitro* cytotoxicity.** HeLa, CaSki, or C33A cells were cultured in 96-well plates (5 × 103 cells/well) for 24 h, then free MG132 or MG132/m were added to each well at various

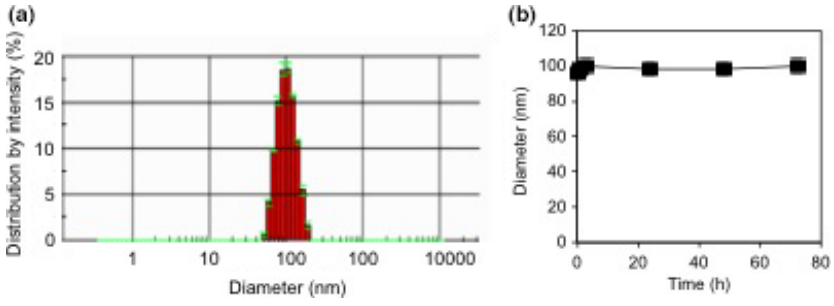

Fig. 2. (a) Size distribution of MG132-loaded polymeric micelles. (b) Changes in the diameter of MG132-loaded polymeric micelles incubated in cell culture media containing 10% FBS at 37°C.

concentrations. The cells were further incubated for 48 h. The cell viability was measured by using a CCK8 kit (Dojindo, Tokyo, Japan) through UV absorption at 480 nm. The cytotoxicity of the drugs was expressed as the 50% inhibitory concentration.

Results

Characterization of MG132/m. To obtain MG132/m, MG132 and PEG-*b*-PBLG were mixed in DMAc, and this mixture was dialyzed against water. The formation of narrowly distributed micellar assemblies (Fig. 1) with Z-average diameters of approximately 100 nm (Fig. 2a) was confirmed by DLS. The drug content in the micelles was found to be 20% in weight, as determined by UV absorption of MG132 at 250 nm after disrupting the micelles in DMAc. MG132-loaded micelles were stable in cell culture media plus 10% FBS at 37°C for more than 3 days, maintaining their size throughout the experiment (Fig. 2b). Under similar conditions, no drug release was observed, suggesting the stable drug loading of MG132/m. We also tested the *in vitro* cytotoxicity of free MG132 and MG132/m against HeLa, CaSki, and C33A cells. The results showed that the micelles were 10-fold less cytotoxic than free MG132, probably because free MG132 is rapidly internalized by the cancer cells to exert its antitumor effect, whereas MG132/m may require more time to kill the cancer cells due to their slow internalization by endocytosis and gradual discharge of the payload (Table 1).

Table 1. Fifty-percent inhibitory concentration (IC_{50}) of free MG132 and MG132-loaded polymeric micelles (MG132/m) against HeLa, CaSki, and C33A cervical cancer cells after 48 h of incubation

Drug	IC_{50}, μM†		
	HeLa	CaSki	C33A
MG132	2.1 ± 1.5	3.2 ± 1.2	5.2 ± 1.1
MG132/m	18.2 ± 3.3	22.4 ± 2.2	23.5 ± 1.5

†Determined by cell counting kit (n = 2).

***In vivo* antitumor activity of MG132/m.** The *in vivo* antitumor activity of free MG132 and MG132/m against cervical cancer was examined using s.c. xenograft models. The drugs were injected at 1 mg/kg on a MG132 base using the following schedule: (i) days 1, 4, 8, 12, 15 18, 23, and 26 for mice bearing HeLa tumors; (ii) days 1, 4, 8, 12, 15 19, 23, and 26 for mice bearing CaSki tumors; and (iii) 1, 4, 8, 12, 15 19, 22,

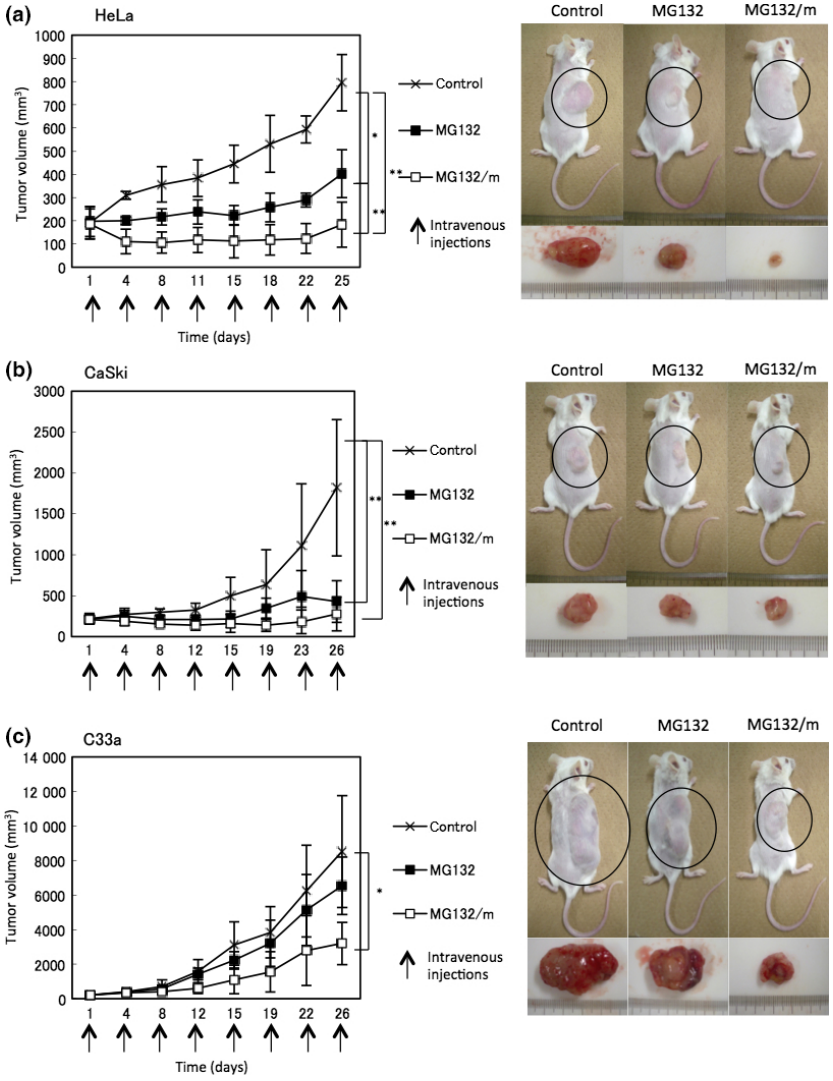

Fig. 3. *In vivo* antitumor effect of MG132 and MG132-loaded polymeric micelles (MG132/m) on human papillomavirus-positive cervical tumors, HeLa (a) and CaSki (b), and human papillomavirus-negative cervical cancer C33A (c). MG132 at 1 mg/kg and MG132/m at 1 mg/kg on a MG132 base were injected i.v. (arrows). Data expressed as the mean ± SD. Statistical significance determined by Student's *t*-test. *$P < 0.05$; **$P < 0.01$.

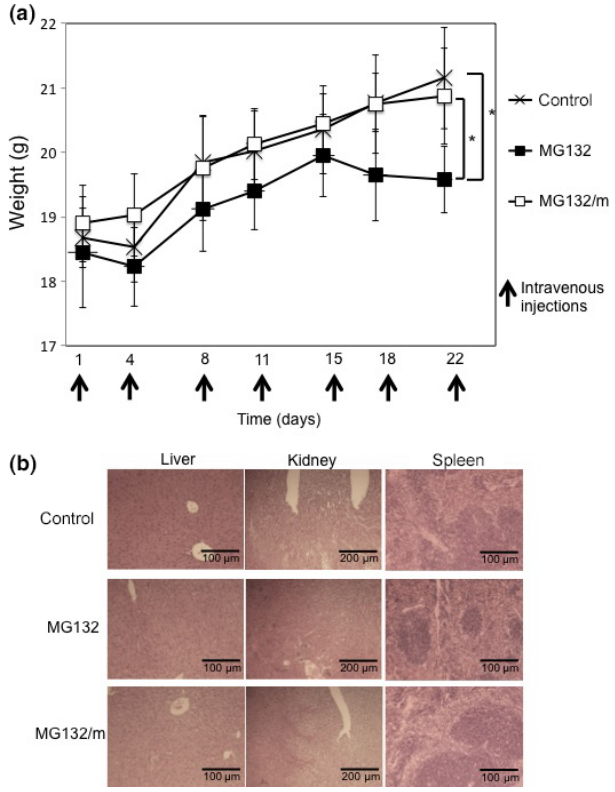

Fig. 4. Toxicity evaluation of MG132 and MG132-loaded polymeric micelles (MG132/m) by weight gains and organ histopathological changes in healthy BALB/c mice. (a) Changes in weight during injection of saline, MG132, or MG132/m twice a week for 4 weeks at 1 mg/kg (seven injections in total; black arrows). Data are mean ± SD ($n = 4$). *$P < 0.05$, Student's *t*-test. (b) Histopathology of organs of control mice (upper panels) and mice after injection of MG132 (middle panels) or MG132/m (lower panels) twice a week for 4 weeks at 1 mg/kg (seven injections in total).

and 26 for mice bearing C33A tumors. The tumor size was measured by a caliper from day 1. The HPV-18-positive HeLa, HPV-16-positive CaSki and HPV-negative C33A cell lines were inoculated in SCID mice ($n = 6$). In HeLa tumors, the growth inhibition rates of MG132 and MG132/m compared to control were 49% ($P < 0.05$) and 77% ($P < 0.01$), respectively, and MG132/m had increased tumor growth inhibitory activity compared to MG132 ($P < 0.01$) (Fig. 3a). In CaSki tumors, MG132/m showed enhanced tumor growth inhibitory effect (85%, control *vs* MG132/m) compared to free MG132 (75%, control *vs* MG132) (Fig. 3b). In addition, MG132/m showed significant growth inhibitory effects (64%, control *vs* MG132/m) against HPV-negative cell line, C33A, compared to free MG132 (24%, control *vs* MG132) (Fig. 3c).

Toxicity of MG132 and MG132/m. Toxicities were estimated by the weight gain of mice without tumors, as well as by histopathological changes in organs. Mice were treated following the same dosing schedule used in the antitumor activity studies. After treatment, the weight gain of the MG132/m group of mice was comparable to that of control group mice, whereas the total weight gain of mice receiving free MG132 was significantly lower than the other two groups ($P < 0.05$) (Fig. 4a). The histopathological analysis of liver, kidney, and spleen in mice treated with saline, free MG132, and MG132/m showed no difference between groups (Fig. 4b).

Fluorescence immunohistochemistry. The expression levels of p53 and hScrib, which are the degradation targets of tumor progression proteins of HPV, were analyzed by immunofluorescence study. The *in vivo* treatment of HeLa and CaSki with proteasome inhibitor resulted in the recovery of the expression of p53 in the nuclei and hScrib in the cellular membrane. In HeLa tumors (Fig. 5a), the expressions of p53 and hScrib were significantly higher when treated with MG132/m compared to free MG132 (Fig. 5b). In CaSki tumors (Fig. 5a,c), p53 and hScrib levels in the MG132/m-treated group were also significantly greater than those in MG132-treated group, although the

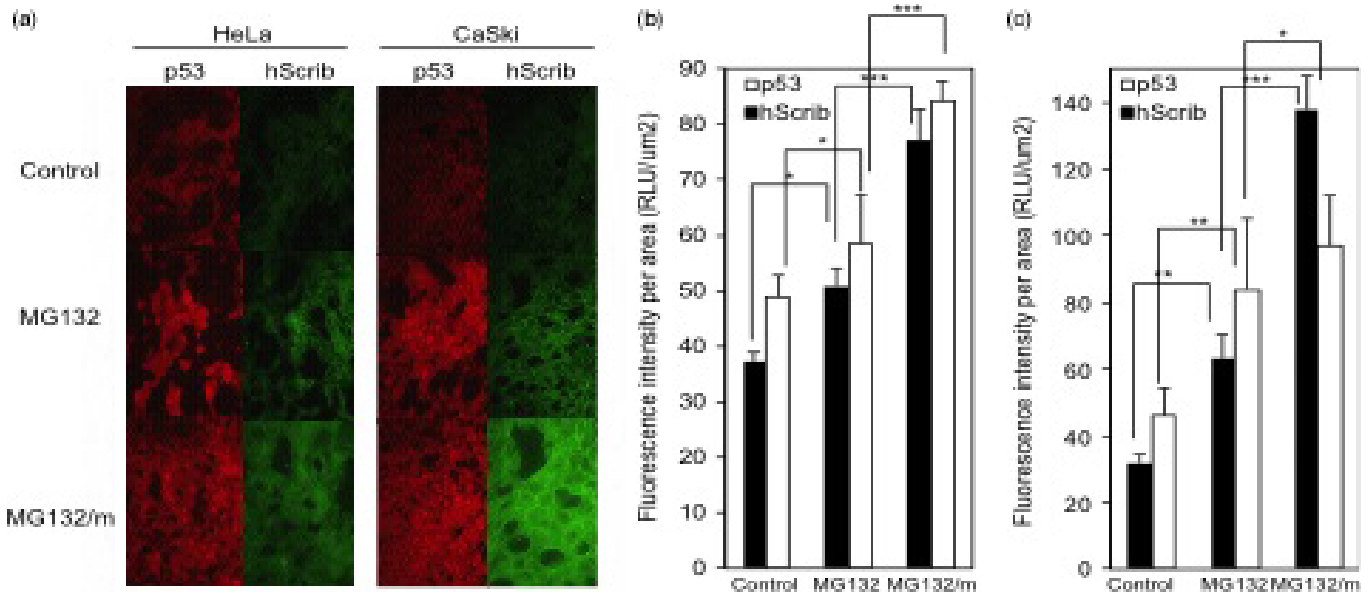

Fig. 5. (a) Expression of p53 (red) and human Scribble (hScrib; green) in HeLa and CaSki cervical tumor xenografts 24 h after i.v. injection of MG132 or MG132-loaded polymeric micelles (MG132/m) (1 mg/kg on a MG132 base) determined by fluorescence immunohistochemistry. (b,c) Quantification of the fluorescence signal from p53 (white) and hScrib (black) in HeLa tumors (b) and in CaSki tumors (c). Data expressed as the mean ± SD ($n = 3$). *$P < 0.05$; ***$P < 0.001$, Student's *t*-test. RLU, relative light unit.

difference in p53 intensity between free MG132 and MG132/m was at the limit of significance ($P = 0.048$). The enhanced expression of p53 and hScrib by micelles was well correlated with their improved therapeutic activity against HeLa and CaSki tumors.

The apoptotic change occurring in HeLa and CaSki xenografts after injecting MG132 or MG132/m was analyzed by TUNEL assay. The number of TUNEL-positive cells was significantly higher in xenografts treated by MG132/m than free MG132 for both HeLa and CaSki tumors (Fig. 6); however, the superior apoptotic levels induced by MG132/m were more evident in HeLa tumors ($P < 0.001$ *vs* free MG132) than in CaSki tumors ($P < 0.05$ *vs* free MG132). It is important to note that, for the immunofluorescence studies, mice received only one injection and the tumors were collected 24 h later but, in the antitumor activity experiment, mice received repeated drug treatment, which may have provided a sufficient therapeutic effect to free MG132 in CaSki tumors to approach the antitumor activity of MG132/m (Fig. 3b).

The increase in the expression of tumor suppressor proteins followed by apoptotic changes in tumor cells may be one of the antitumor mechanisms of proteasome inhibitors against cervical cancers.

Blood circulation of MG132/m. To analyze the blood circulation of MG132/m, a fluorescent dye, BODIPY TR, was conjugated to MG132 for tracking the fluorescent signal. Preparation of MG132-BODIPY-loaded micelles was similar to that of MG132/m. Free MG132-BODIPY and MG132-BODIPY micelles were injected into the tail vein of mice. Blood circulation and accumulation into the tumor was evaluated by intravital microscopy (Fig. 7a). The fluorescent signal intensities taken from each ROI were normalized to the initial intensity. Results showed that free MG132-BODIPY was rapidly eliminated from blood circulation within 10 min of injection, and was not retained in tumor tissue (Fig. 7). Conversely, MG132-BODIPY micelles stayed in the blood circulation for a prolonged time, and their accumulation in tumor gradually increased for hours (Fig. 7b), in agreement with the EPR effect.

Tumor accumulation and tissue distribution. HeLa-GFP xenografts were analyzed 24 h after injecting free MG132-BODIPY or MG132-BODIPY/m. As shown in Figure 8, MG132/m achieved 3-fold higher accumulation than free MG132 (97.3 *vs* 31.4) in HeLa tumors. As for other organs, signals from MG132-BODIPY/m appeared in the excretory and metabolic organs like liver, spleen, and kidney were more than that from free MG132-BODIPY, which is associated with the increased bioavailability of the micelles. MG132- BODIPY/m did not show higher accumulation into brain, lung, or muscle than free MG132-BODIPY (Fig. 9). The highest accumulation of

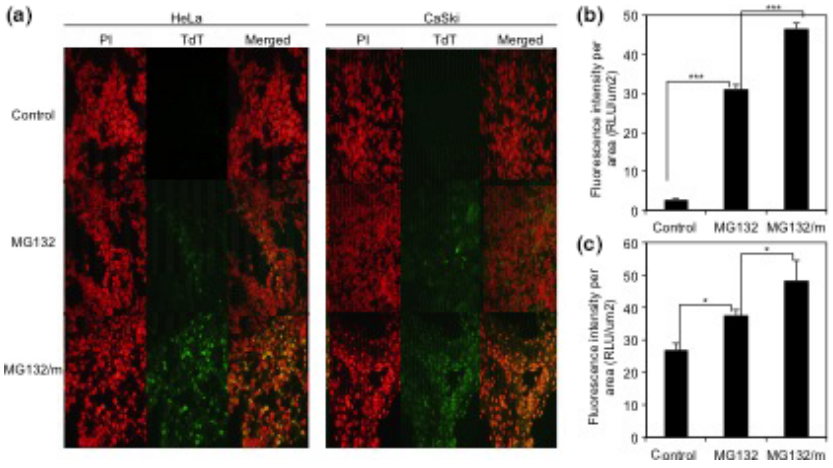

Fig. 6. (a) Apoptotic levels in HeLa and CaSki cervical tumor xenografts analyzed by TUNEL assay 24 h after i.v. injection of MG132 or MG132-loaded polymeric micelles (MG132/m) (1 mg/kg on a MG132 base). Green, terminal deoxynucleotidyl transferase (TdT); red, propidium iodide (PI); yellow, colocalization. (b) Quantification of the fluorescence signal from TdT in HeLa tumors. (c) Quantification of the fluorescence signal from TdT in CaSki tumors. Data expressed as the mean ± SD ($n = 3$). *$P < 0.05$; ***$P < 0.001$, Student's *t*-test.

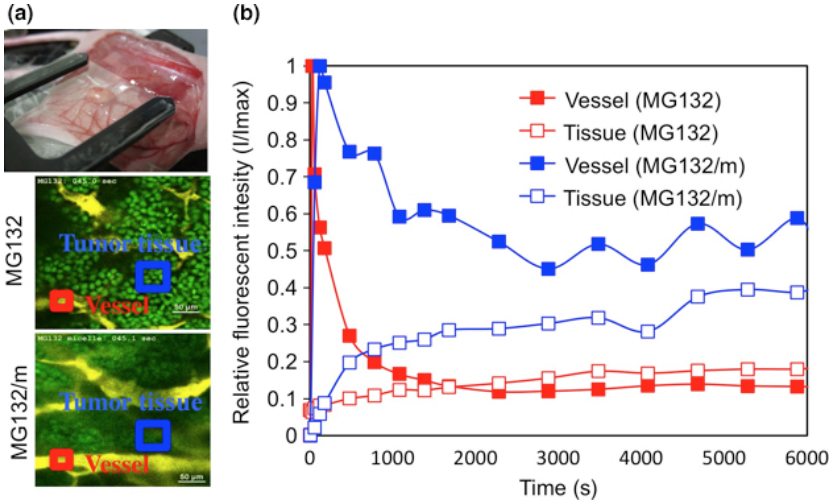

Fig. 7. Intratumoral microdistribution of fluorescent-labeled MG132 (MG132-BODIPY) and MG132-loaded polymeric micelles (MG132/m) (MG132-BODIPY/m). (a) Skin flap of a HeLa-GFP xenograft was placed under cover glass for analysis with microscope (upper panel). The microscopic field of view (645.5 × 645.5 μm) showed HeLa-GFP cells (green), and MG132-BODIPY (yellow; center panel) or MG132-BODIPY/m (yellow; lower panel). Two regions of interest were selected in an artery (red box) and tumor (blue box) for analysis of the circulation and accumulation of MG132-BODIPY and MG132-BODIPY/m, respectively. (b) Time profiles of the fluorescent signals in these regions of interest. The fluorescent signals were normalized to the maximum fluorescence of each drug observed in blood at the injection point.

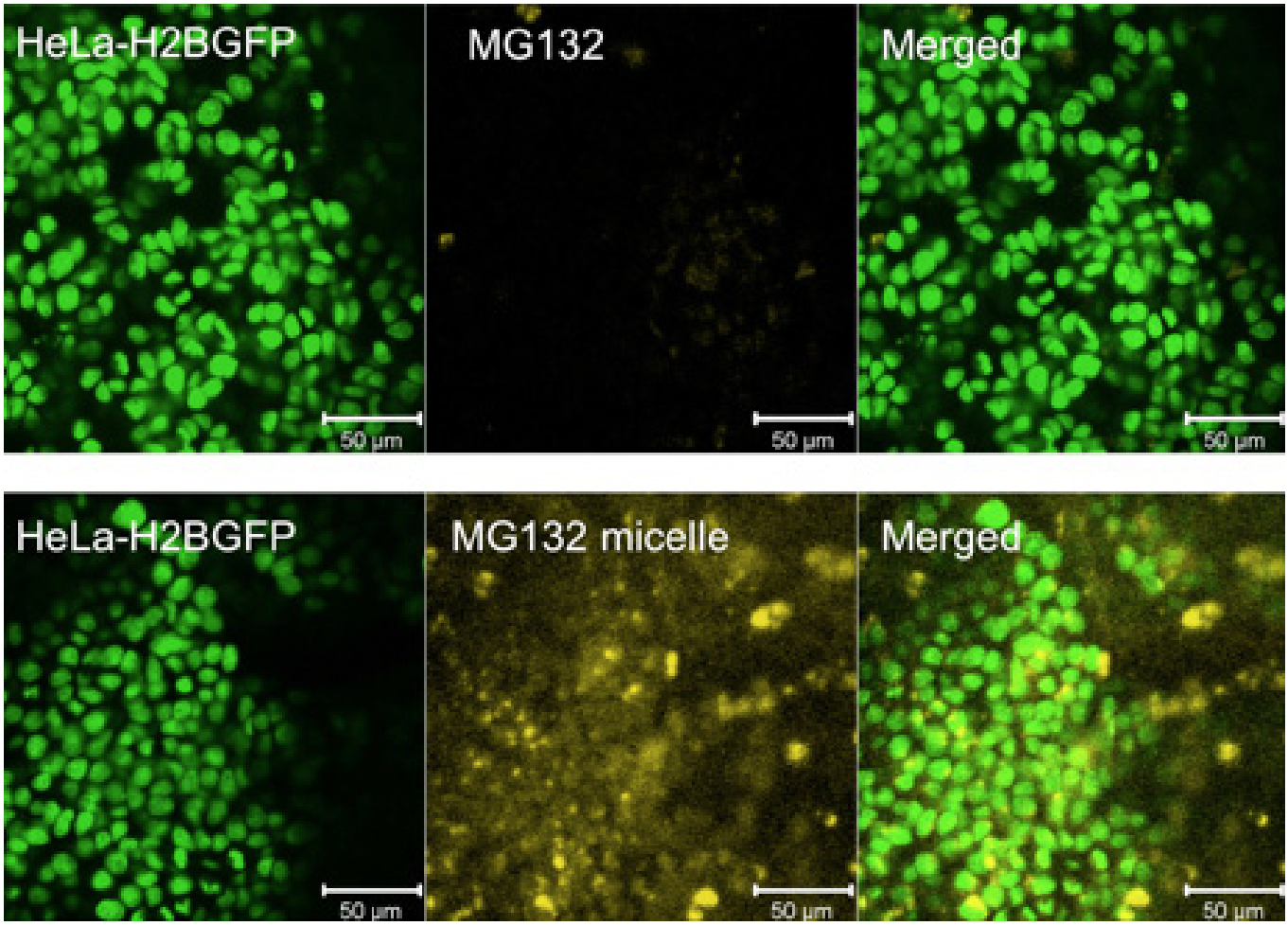

Fig. 8. Distribution of fluorescent-labeled MG132 (yellow; upper panels) and MG132-loaded polymeric micelles (yellow; lower panels) in HeLa-GFP tumors (green) in mice, determined by confocal microscopy. Images were acquired 24 h after injection of the drugs.

MG132-BODIPY/m was observed in liver, which can be associated with the scavenging of nanoparticulate materials in this organ. Moreover, the accumulation of MG132-BODIPY/m in kidney could be related to the partial leakage of the drug from the micelles in the bloodstream, comparable to other polymeric micelles physically entrapping hydrophobic drugs.[15]

In addition, although the conjugation of a fluorescent probe to MG132 may affect the pharmacokinetics and tissue distribution, our results clearly indicate the enhanced bioavailability of the drug and superior accumulation in tumor tissues by delivery through polymeric micelles.

Discussion

Our findings illustrate the potential of using polymeric micelles incorporating proteasome inhibitors for improving their antitumor efficacy against cervical cancers. The core-shell architecture of MG132/m allowed high physical loading of the hydrophobic drug in the core of the micelles (20% in weight), while protecting the cargo from degradation in the bloodstream. Moreover, the extended blood circulation of MG132/m served their accumulation in solid tumors and increased their antitumor effect. The real-time microscopy data confirmed the difference in distribution in the bloodstream and cancer tissue of free MG132 and MG132/m, which gradually accumulated in tumors for hours, corresponding with the EPR effect.

MG132-loaded micelles showed significant tumor growth inhibition against HPV-positive HeLa and CaSki tumors, and the recoveries of tumor suppressor proteins and populations of apoptotic cells in the tumors correlated with their enhanced activity. We have previously reported for that the strong antitumor effect of proteasome inhibitor bortezomib (PS-341) against HeLa and CaSki tumors was associated with the recovery of p53 and apoptotic cell rates. Moreover, the efficacy of bortezomib could be further enhanced when combined with cisplatin, with the bortezomib/cisplatin combination showing the highest recovery of tumor suppressor proteins.[6] These results support the role of the recovery of degradation target proteins of HPV in the enhanced antitumor effect of MG132/m against cervical cancer, but also suggests the possibility of co-administering MG132/m with cisplatin for developing synergistic therapies against cervical cancer. Our data also showed that MG132/m had significant antitumor activity against HPV-negative cervical cancer cell line C33A. *In vitro* expressions of p53 and hScrib in HeLa, CaSki, and C33A cells exposed to free MG132 were analyzed in advance. Under several exposure times and concentrations, the expression level of p53 and hScrib increased in HeLa and in CaSki cells but did not in C33A cells (Fig. S1). These results suggest that MG132

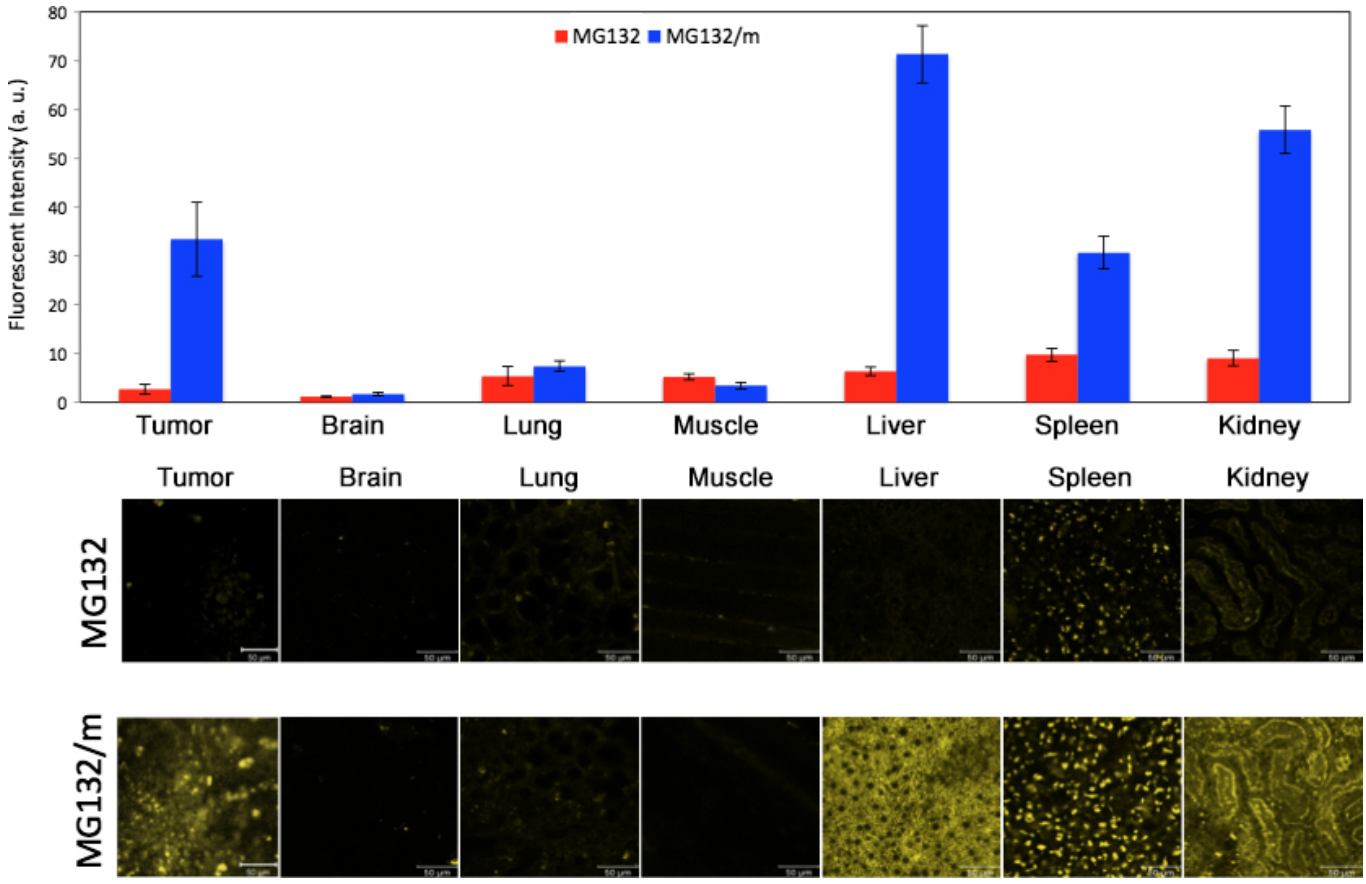

Fig. 9. Quantification of the tissue distribution of fluorescent-labeled MG132 (red columns) and MG132-loaded polymeric micelles (MG132/m; blue columns) from confocal microscopies 24 h after injection into mice (upper panel). Data are mean ± SD (n = 3). Representative fluorescent microscopies are shown in the lower panels.

/m may enhance the antitumor effect of proteasome inhibitors not only by the recovery of HPV-related tumor suppressor proteins, but also through a different mechanism, as many proteasome substrates are known to be mediators of pathways that are dysregulated in neoplasia. Indeed, several reports have indicated that proteasomes are involved in cell cycle regulation by cyclin-dependent kinase complexes, cell cycle arrest, and DNA repair by the p53–MDM2 pathway (MDM2 is a ubiquitin ligase E3 for p53), the nuclear factor-κB pathway for cell growth, angiogenesis, or susceptibility to chemotherapeutic agents and caspase dependent-apoptosis.[22–27] Thus, enhanced accumulation of MG132 delivered by the micelles in C33A cells may allow effective suppression of these pathways with some thresholds for action. Future work will be needed to reveal the mechanisms involved in the enhanced intracellular availability of active MG132 delivered by micelles.

Our previously reported MG132-loaded micelles, which have the drug integrated to the nanostructure by covalent binding for specific release at endosomal pH, exerted antitumor effects at doses higher than 16 mg/kg on a MG132 base against s.c. HeLa tumors.[28] In this study, we developed MG132/m that physically load the proteasome inhibitor and achieved strong suppression of the tumor growth even at 1 mg/kg on a MG132 base, suggesting high potency *in vivo*. This increase in efficacy of MG132/m did not reduce their safety, and the micelles could be injected repeatedly, with the mice gaining weight as much as controls after treatment with MG132/m injections with no histological damage in organs in which MG132/m accumulates, such as liver, kidney, and spleen. The safety of polymeric micelles, such as NK105 (paclitaxel-incorporated polymeric micelles),[17,29] NC-6004 (cisplatin-incorporated micelles),[30] and NK012 (SN-38-incorporated micelles),[31] has been reported in clinical trials. Like MG132/m, NK105 incorporates the drug in the core by hydrophobic interaction with the core-forming segment.[29] The clinical trial of NK105 showed that these micelles could be safely infused in patients, with the paclitaxel loaded in the micelles having a 15-fold higher plasma area under the concentration time curve than that of conventional paclitaxel dosage and without any patient experiencing grade 3/4 hypersensitive reactions. The trial confirmed the safety of polymeric micelles designed for stably incorporating anticancer agents by physical forces.

We have shown that polymeric micelles can successfully enhance the performance of the proteasome inhibitor MG132 against cervical cancers. As the inhibition of proteasomes has a wide variety of activities and functions in cell control, micellar formulations of MG132 could be further applied for the targeted treatment of other malignancies.

Acknowledgments

This work was supported by Grants-in-Aid for Scientific Research from the Ministry of Education, Culture, Sports, Science and Technology of Japan (21791542) (Yoko Matsumoto), the Banyu Research Grant for Female Researchers (Yoko Matsumoto), the Center of Innovation Program from the Japan Science and Technology Agency (Nobuhiro

Nishiyama), the Project for Development of Innovative Research on Cancer Therapeutics (P-Direct) and Practical Research for Innovative Cancer Control from the Japan Agency for Medical Research and Development (both Nobuhiro Nishiyama).

Disclosure Statement

The authors have no conflict of interest.

Abbreviations

DLS	dynamic light scattering
DMAc	dimethyl acetamide
DMF	*N*,*N*-dimethylformamide
EPR	enhanced permeability and retention
HPV	human papillomavirus
hScrib	human Scribble
MWCO	molecular weight cut-off of the membrane
MG132/m	MG132-loaded micelles
PEG-*b*-PBLG	PEG-*b*-poly(γ-benzyl-L-glutamate)
ROI	region of interest
UPS	ubiquitin proteasome system

References

1 Ferlay J, Shin HR, Bray F, Forman D, Mathers C, Parkin DM. *BLOBOCAN 2008v2.0*, in *Cancer Incidence and Mortality Worldwide: IARC CancerBase No. 10 [Internet]*, International Agency for Research on Cancer, Lyon, France, 2010. [cited 1 April 2013.] Available from URL: http://globocan.iarc.fr.
2 Berek JS, Neville Hacker F. *Practical Gynecologic Oncology*, 4th edn. New York, NY: Lippincott Williams & Wilkins, 2005.
3 Nakagawa S, Yoshikawa H, Yasugi T *et al.* Ubiquitous presence of E6 and E7 transcripts in human papillomavirus-positive cervical carcinomas regardless of its type. *J Med Virol* 2000; **62**(2): 251–8.
4 Comerford SA, Maika SD, Laimins LA, Messing A, Elsasser HP, Hammer RE. E6 and E7 expression from the HPV 18 LCR: development of genital hyperplasia and neoplasia in transgenic mice. *Oncogene* 1995; **10**: 587–97.
5 Huibregtse JM, Scheffner M, Howley PM. Cloning and expression of the cDNA for E6-AP, a protein that mediates the interaction of the human papillomavirus E6 oncoprotein with p53. *Mol Cell Biol* 1993; **13**(2): 775–84.
6 Miyamoto Y, Nakagawa S, Wada-Hiraike O *et al.* Sequential effects of the proteasome inhibitor bortezomib and chemotherapeutic agents in uterine cervical cancer cell lines. *Oncol Rep* 2013; **29**(1): 51–7.
7 Kamer S, Ren Q, Dicker AP. Differential radiation sensitization of human cervical cancer cell lines by the proteasome inhibitor velcade (bortezomib, PS-341). *Arch Gynecol Obstet* 2009; **279**(1): 41–6.
8 Kane RC, Bross PF, Farrell AT, Pazdur R. Velcade: U.S. FDA approval for the treatment of multiple myeloma progressing on prior therapy. *Oncologist* 2003; **8**: 508–13.
9 Moreau P, Pylypenko H, Grosicki S *et al.* Subcutaneous versus intravenous administration of bortezomib in patients with relapsed multiple myeloma: a randomised, phase 3, non-inferiority study. *Lancet Oncol* 2011; **12**: 431–40.
10 Mukai H, Ohyashiki K, Katoh T *et al.* Lung injury associated with bortezomib therapy in Japan. *Rinsho Ketsueki* 2011; **52**: 1859–69.
11 Matsumura Y. Polymeric micellar delivery systems in oncology. *Jpn J Clin Oncol* 2008; **38**: 793–802.
12 Matsumura Y, Maeda H. A new concept for macromolecular therapeutics in cancer chemotherapy: mechanism of tumoritropic accumulation of proteins and the antitumor agent smancs. *Cancer Res* 1986; **46**(12 Pt 1): 6387–92.
13 Yokoyama M, Miyauchi M, Yamada N *et al.* Preparation of micelle-forming polymer-drug conjugates. *Bioconjug Chem* 1992; **3**: 295–301.
14 Nishiyama N, Okazaki S, Cabral H *et al.* Novel cisplatin-incorporated polymeric micelles can eradicate solid tumors in mice. *Cancer Res* 2003; **63**: 8977–83.
15 Cabral H, Kataoka K. Progress of drug-loaded polymeric micelles into clinical studies. *J Control Release* 2014; **190**: 465–76.
16 Matsumura Y. Poly (amino acid) micelle nanocarriers in preclinical and clinical studies. *Adv Drug Deliv Rev* 2008; **60**: 899–914.
17 Kato K, Chin K, Yoshikawa T *et al.* Phase II study of NK105, a paclitaxel-incorporating micellar nanoparticle, for previously treated advanced or recurrent gastric cancer. *Invest New Drugs* 2012; **30**: 1621–7.
18 Crook T, Wrede D, Vousden KH. p53 point mutation in HPV negative human cervical carcinoma cell lines. *Oncogene* 1991; **6**: 873–5.
19 Kanda T, Sullivan KF, Wahl GM. Histone-GFP fusion protein enables sensitive analysis of chromosome dynamics in living mammalian cells. *Curr Biol* 1998; **8**: 377–85.
20 Cabral H, Matsumoto Y, Mizuno K *et al.* Accumulation of sub-100 nm polymeric micelles in poorly permeable tumours depends on size. *Nat Nanotechnol* 2011; **6**: 815–23.
21 Matsumoto Y, Nomoto T, Cabral H *et al.* Direct and instantaneous observation of intravenously injected substances using intravital confocal microvideography. *Biomed Opt Express* 2010; **1**: 1209–16.
22 Han YH, Moon HJ, You BR, Park WH. The effect of MG132, a proteasome inhibitor on HeLa cells in relation to cell growth, reactive oxygen species and GSH. *Oncol Rep* 2009; **22**(1): 215–21.
23 Miller SC, Huang R, Sakamuru S *et al.* Identification of known drugs that act as inhibitors of NF-kappaB signaling and their mechanism of action. *Biochem Pharmacol* 2010; **79**: 1272–80.
24 Hougardy BM, Maduro JH, van der Zee AG *et al.* Proteasome inhibitor MG132 sensitizes HPV-positive human cervical cancer cells to rhTRAIL-induced apoptosis. *Int J Cancer* 2006; **118**: 1892–900.
25 Rousseau D, Cannella D, Boulaire J, Fitzgerald P, Fotedar A, Fotedar R. Growth inhibition by CDK-cyclin and PCNA binding domains of p21 occurs by distinct mechanisms and is regulated by ubiquitin-proteasome pathway. *Oncogene* 1999; **18**: 4313–25.
26 Adams J. Development of the proteasome inhibitor PS-341. *Oncologist* 2002; **7**(1): 9–16.
27 Laussmann MA, Passante E, Hellwig CT *et al.* Proteasome inhibition can impair caspase-8 activation upon submaximal stimulation of apoptotic tumor necrosis factor-related apoptosis inducing ligand (TRAIL) signaling. *J Biol Chem* 2012; **287**: 14402–11.
28 Quader S, Cabral H, Mochida Y *et al.* Selective intracellular delivery of proteasome inhibitors through pH-sensitive polymeric micelles directed to efficient antitumor therapy. *J Control Release* 2014; **188**: 67–77.
29 Hamaguchi T, Matsumura Y, Suzuki M *et al.* NK105, a paclitaxel-incorporating micellar nanoparticle formulation, can extend *in vivo* antitumour activity and reduce the neurotoxicity of paclitaxel. *Br J Cancer* 2005; **92**: 1240–6.
30 Uchino H, Matsumura Y, Negishi T *et al.* Cisplatin-incorporating polymeric micelles (NC-6004) can reduce nephrotoxicity and neurotoxicity of cisplatin in rats. *Br J Cancer* 2005; **93**: 678–87.
31 Matsumura Y. Preclinical and clinical studies of NK012, an SN-38-incorporating polymeric micelles, which is designed based on EPR effect. *Adv Drug Deliv Rev* 2011; **63**: 184–92.

Supporting Information

Additional Supporting Information may be found online in the supporting information tab for this article:

Fig. S1. (a) Expression of p53 and human Scribble (hScrib) in cervical cancer cell lines (CaSki, HeLa, and C33A) after exposure to 1 μM free MG132 in cell culture media containing 10% FBS at 37°C for 0 (control), 3, 12, and 24 h.